Nuclear magnetic resonance study of the magnetic-field-induced ordered phase in the NiCl$_2$-4SC(NH$_2$)$_2$ compound

Rémi Blinder,[1,*] Maxime Dupont,[2] Sutirtha Mukhopadhyay,[1,†] Mihael S. Grbić,[1,3] Nicolas Laflorencie,[2] Sylvain Capponi,[2] Hadrien Mayaffre,[1] Claude Berthier,[1] Armando Paduan-Filho,[4] and Mladen Horvatić[1,‡]

[1]*Laboratoire National des Champs Magnétiques Intenses, LNCMI-CNRS (UPR3228), EMFL, UGA, UPS, and INSA, Boîte Postale 166, 38042, Grenoble Cedex 9, France*

[2]*Laboratoire de Physique Théorique, IRSAMC, Université de Toulouse, CNRS, 31062 Toulouse, France*

[3]*Department of Physics, Faculty of Science, University of Zagreb, Bijenička 32, Zagreb HR 10000, Croatia*

[4]*Instituto de Física, Universidade de São Paulo, 05315-970 São Paulo, Brazil*

Nuclear magnetic resonance study of the high magnetic field (H) part of the Bose-Einstein condensed (BEC) phase of the quasi-one-dimensional (quasi-1D) antiferromagnetic quantum spin-chain compound NiCl$_2$-4SC(NH$_2$)$_2$ was performed. We precisely determined the phase boundary, $T_c(H)$, down to 40 mK; the critical boson density, $n_c(T_c)$; and the absolute value of the BEC order parameter $S_\perp$ at very low temperature ($T = 0.12$ K). All results are accurately reproduced by numerical quantum Monte Carlo simulations of a realistic three-dimensional (3D) model Hamiltonian. Approximate analytical predictions based on the 1D Tomonaga-Luttinger liquid description are found to be precise for $T_c(H)$, but less so for $S_\perp(H)$, which is more sensitive to the strength of 3D couplings, in particular close to the critical field. A mean-field treatment, based on the Hartree-Fock-Popov description, is found to be valid only up to $n_c \cong 4\%$ ($T < 0.3$ K), while for higher n_c boson interactions appear to modify the density of states.

DOI: 10.1103/PhysRevB.95.020404

Quantum phase transitions, i.e., phase transitions that are driven by quantum, rather than thermal, fluctuations, are one of the topical subjects in condensed matter physics [1–4]. There are numerous experimental investigations of such transitions as a function of an external control parameter, such as magnetic field (H), pressure, or chemical composition. The NiCl$_2$-4SC(NH$_2$)$_2$ (DTN) quantum magnet has long been studied in this respect [5–11]. The system consists of weakly coupled chains of $S = 1$ spins, borne by Ni^{2+} ions, subject to the Hamiltonian [8]

$$\mathcal{H} = \sum_{\boldsymbol{r}} \left\{ \sum_{v=a,b,c} J_v \hat{\boldsymbol{S}}_{\boldsymbol{r}} \cdot \hat{\boldsymbol{S}}_{\boldsymbol{r}+\boldsymbol{v}} \right\} + D(\hat{S}_{\boldsymbol{r}}^z)^2 - g\mu_B H \hat{S}_{\boldsymbol{r}}^z, \quad (1)$$

where summations are performed over all lattice positions ($\boldsymbol{r}$) and unit cell vectors ($\boldsymbol{v}$). Equation (1) shows that the spins are subject to an easy-plane anisotropy [the $D(\hat{S}_{\boldsymbol{r}}^z)^2$ term, where $D/k_B = 8.9$ K] and the nearest-neighbor Heisenberg interaction ($J_v \hat{\boldsymbol{S}}_{\boldsymbol{r}} \cdot \hat{\boldsymbol{S}}_{\boldsymbol{r}+\boldsymbol{v}}$), preferentially along the chain (c-axis direction), $J_c/k_B = 2.2$ K. Also, an interchain coupling $J_{ab}/k_B = 0.18$ K is present, which, because of the tetragonal symmetry, is equivalent for the a and b directions. As the antiferromagnetic (AF) couplings differ by an order of magnitude ($J_c/J_{ab} \cong 12$), the system can be considered as quasi-one-dimensional (quasi-1D). Between critical fields $H_{c1} = 2.1$ T and $H_{c2} = 12.32$ T [6,7,9], and at low temperature (T) it displays a three-dimensional (3D) AF ordered phase

that can be described as a Bose-Einstein condensation (BEC) of the spin degrees of freedom (belonging to the 3D XY universality class) [12]. In the BEC phase a transverse AF magnetic moment develops, corresponding to the BEC order parameter [12–15]. Although the existence of such a state is intrinsically a 3D phenomenon, a pronounced 1D character is known to affect some of its properties in a nontrivial and interesting way [16,17]. The spin ladders CuBr$_4$(C$_5$H$_{12}$N)$_2$ (BPCB) [17,18] and (C$_7$H$_{10}$N$_2$)CuBr$_4$ [19–21], whose anisotropy of coupling constants (1D character) is ~10 times stronger than in DTN, were successfully described using the 1D Tomonaga-Luttinger liquid (TLL) framework [22], enhanced by considering the transverse couplings [16–18], which induce a long-range order at finite temperature. We recall here that both Hamiltonians of a spin-1 chain in the $D \gg J_c$ limit and a spin-1/2 ladder in the $J_{\text{rung}} \gg J_{\text{leg}}$ limit can be reduced, for low temperature, to the same basic XXZ spin-1/2 chain model and are thus equivalent—as much as the strong D and J_{rung} limits are respected [9]. In a previous work, DTN and BPCB were indeed found to show equivalent spin dynamics in the quantum critical regime [seen through the nuclear magnetic resonance (NMR) T_1 relaxation time] [9]. However, the correctness of the TLL approach for a system which is less 1D than the above-mentioned two spin-ladder compounds has not been specifically addressed so far, and was only very recently discussed regarding NMR relaxation (dynamic) properties [23]. This question is here addressed by an NMR study of static properties of DTN, in the field close to H_{c2} (the transition to the fully polarized phase), in which (1) we have accurately determined the *absolute* value of the order parameter (that is, the transverse, AF spin component $S_\perp$) in the BEC phase; (2) our low temperature (down to 40 mK) NMR data for the T-H phase boundary are compatible with the theoretically expected behavior for the zero-T limit, $T_c(H) \propto (H_{c2} - H)^{2/3}$, in contrast to previously published results [24];

---

*Present address: CEA, INAC, SPRAM (UMR5819 CEA/CNRS/UJF), 17 rue des Martyrs, 38054 Grenoble cedex 9, France.

†Present address: BAT-SOL Equipment and Technology, Vashi, Navi Mumbai – 400 705, India.
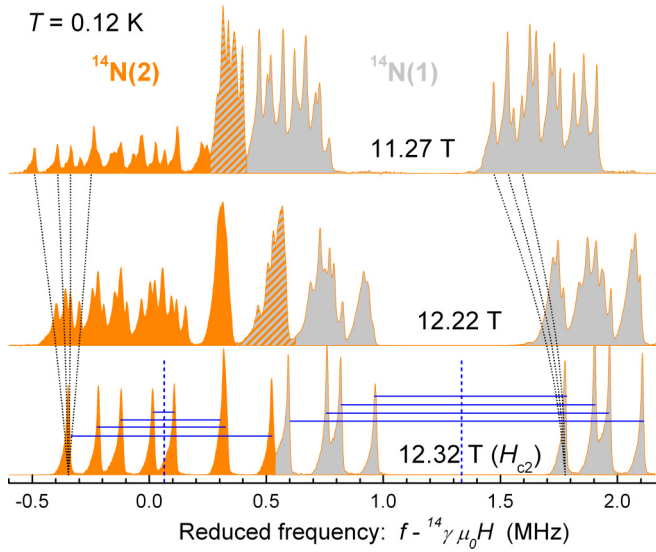
‡mladen.horvatic@lncmi.cnrs.fr

FIG. 1. Evolution of ^{14}N NMR spectrum when entering the BEC phase in DTN at $T = 0.12$ K. In the spectrum taken at $H_{c2} = 12.32$ T (bottom), the contributions from the two crystallographic sites, orange-colored N(2) and gray-colored N(1), are clearly separated, and the quadrupolar splittings, indicated by blue horizontal lines, are easy to identify. Within the ordered phase, at 12.22 and 11.27 T, the AF order splits each line into four, as shown on the lowest frequency N(2) line by the dotted curves. Orange-gray hatching denotes the region where the N(2) and N(1) lines overlap.

and (3) we also determined the sample magnetization at T_c and thus the critical boson density, complementing the already existing data close to H_{c1} [25]. The complete set of experimental data is accurately reproduced by numerical quantum Monte Carlo (QMC) simulations for the standard 3D $S = 1$ model of Eq. (1). This method is computationally quite demanding, but provides a reliable basis to discuss the validity of simpler (approximate) analytical predictions, within either TLL theory or a mean-field Hartree-Fock-Popov (HFP) description [14]. Unlike in the previously studied spin ladders, where the 3D (interladder) couplings were taken as a free adjustable parameter to fit the experimental T_c values, in DTN these couplings have been determined independently [8,10], making the theoretical description fully constrained and able to predict the absolute values of observables.

Experiments were performed on a DTN single crystal of dimensions $\sim 2 \times 2 \times 3$ mm^3, placed inside the mixing chamber of a dilution refrigerator, by NMR of proton ^{1}H (nuclear spin $I = 1/2$) and nitrogen ^{14}N ($I = 1$) nuclei. The local magnetization (spin polarization) of magnetic (Ni^{2+}) ions, polarized by the applied magnetic field H, is "seen" by NMR nuclei as an additional local field δH and the corresponding NMR frequency $f = \gamma \mu_0 |H + \delta H|/(2\pi)$, where γ is the gyromagnetic factor [26,27]. The observed asymmetric line shape of each individual line in the NMR spectrum (Fig. 1) is well explained by the inhomogeneity of the demagnetizing field over the sample volume [28]. ^{14}N nuclei, in addition, experience the so-called *quadrupolar* coupling to the local electric field gradient (EFG) tensor [26,27] which strongly splits each NMR line in two (Fig. 1). This splitting has dramatic variations when the sample is rotated, thus allowing
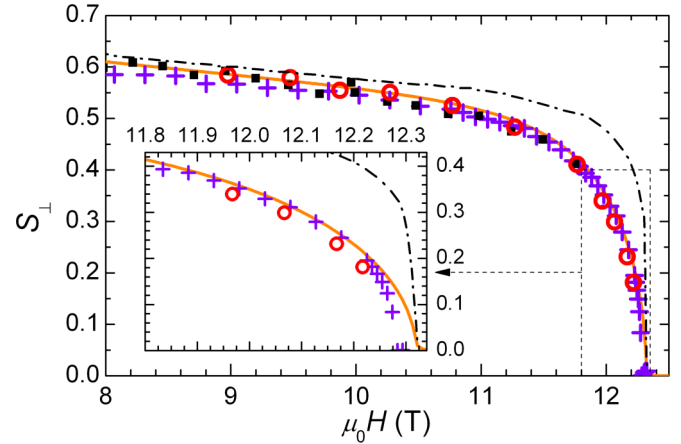

FIG. 2. The order parameter ($S_\perp$) in the BEC phase of DTN at $T = 0.12$ K determined by NMR (circles) and by QMC simulations (crosses). NMR points are overlapped by neutron diffraction data from Ref. [10] downscaled by -25% (squares). The orange solid line and dashed-dotted black curve are the $T = 0$ prediction by DMRG+MF and by TLL+MF, respectively. The inset shows a zoom close to H_{c2}.

precise *in situ* determination of the complete EFG tensor and consequently of the sample orientation (for details, see Ref. [28]). The c axis of the sample was here tilted by $\theta = 3.1°$ from the field direction. In order to determine the (nearly) zero-temperature value of the order parameter in the BEC phase, nitrogen spectra were recorded at $T = 0.12$ K, a temperature ten times lower than the maximum T_c, $T_c^{\text{max}} = 1.2$ K, and at different magnetic fields 9 T $< H < H_{c2}$ (Fig. 2). Two different ^{14}N signals are observed in the NMR spectrum, attributed to the two nitrogen crystallographic sites N(1) and N(2) [28–30]. On entering the BEC phase, one can observe that the relative intensity of the N(2) lines is decreasing, which is just an artifact of the measurement sequence (effect of the "T_1" relaxation) [31]. More importantly, a transverse spin component $S_\perp$ appears, corresponding to the BEC order parameter. Since $S_\perp$ is AF ordered, it creates a staggered local field at the nuclei, which results in a splitting of each NMR line. In canonical systems, AF order induces a *doubling* of the unit cell, which results in a splitting of each line into two, since the local field takes only two possible values. This is seen in previous NMR studies [18,20]. The situation is somewhat more complex in DTN, which has a body-centered tetragonal (BCT) lattice, corresponding to *two* interpenetrating tetragonal subsystems shifted by half of the tetragonal unit cell [29]. As a result, each NMR line splits into $2 \times 2 = 4$ lines when entering an AF ordered phase (see Supplemental Material (SM) [30]). This line splitting is very difficult to follow in the proton spectra (not shown), because they comprise many overlapping lines, but can be successfully tracked in ^{14}N spectra. Indeed, as soon as H is slightly misaligned from the c axis of tetragonal symmetry, ^{14}N NMR lines are well separated by the quadrupolar effects (Fig. 1), so that the overlap of lines remains tractable.

To convert the observed line splitting into an order parameter, the main issue is to infer hyperfine tensors **A** relating the spin polarization $S_\perp$ to the observed δH. For a *homogeneous*

order, the corresponding $\mathbf{A}(\boldsymbol{q} = \boldsymbol{0})$ at zero wave vector is easily determined from the NMR line shift recorded above H_{c2}, where the system is completely polarized [28]. However, the order parameter $S_\perp$ corresponds to $\mathbf{A}(\boldsymbol{q} = \boldsymbol{q}_{AF})$ at the AF wave vector, whose determination is highly nontrivial (see SM [30] for further details). As for the N(1) site further complications are brought by the strong isotropic component of the $\mathbf{A}$ tensor, we decided to quantitatively analyze only the N(2) data, to finally obtain the *absolute value* of the order parameter *amplitude*. Figure 2 shows these results in comparison with different numerical and theoretical descriptions. The magnetic field dependence of $S_\perp$ observed by NMR is perfectly consistent with what was previously reported from neutron measurements (carried out up to 12 T) [10]. However, in these latter data there is apparently a problem with the determination of the absolute value of $S_\perp$, and we had to downscale them by -25% to make them consistent with the theoretical prediction and the $S_\perp$ values determined by NMR.

QMC simulations were performed for a simple tetragonal lattice, considering the two tetragonal subsystems of DTN as totally decoupled. In reality, the BCT crystal structure of DTN contains two interpenetrating tetragonal subsystems, connected to each other through an additional, geometrically *frustrated* coupling (J_f) [10] that cannot be treated by these simulations. However, corrections to this approximation are expected to be very small, much smaller than the experimentally determined coupling constant, $J_f = 80$ mK [10], because a perfectly frustrated coupling between the two subsystems should have no effect at all at the mean-field level. Indeed, despite the approximation, the QMC simulations (see SM [30] for more details) performed at $T = 0.12$ K agree remarkably well with the experiments.

For a quasi-1D system, a second, computationally less demanding approach to describe the order parameter at $T = 0$, is to take into account the interchain (3D) coupling within a mean-field (MF) approximation, neglecting spin fluctuations. This leads to a model of a single DTN chain in an effective magnetic field having a transverse staggered component due to AF transverse ordering and a longitudinal component due to the magnetization. This model can be exactly solved numerically, in a self-consistent way, using the matrix-product state formalism and density matrix renormalization group (DMRG) algorithm [17,32–34], to find the ground-state ($T = 0$) order parameter. The values obtained in this way, shown in Fig. 2, are very close to those from QMC (calculated at 0.12 K). Note that the apparent overestimate of $S_\perp$ by this DMRG+MF method, of about 3%, is partly due to the difference in the corresponding temperatures. Another possibility to solve this 1D effective model is to use analytical expressions based on an (approximate) TLL approach that includes most relevant bosonized MF terms in the Hamiltonian, leading to [16–18,22]

$$S_\perp = F(K)\sqrt{2A_x}\left(\frac{\pi Z J_{ab} A_x}{u}\right)^{1/(8K-2)}, \qquad (2)$$

where K is the TLL exponent, u is the velocity of the excitations, A_x is the amplitude of the transverse correlation function [35], $Z = 4$ is the coordination number along the

transverse a,b directions, and $F(K)$ is

$$F(K) = \left\{\frac{\frac{8K\pi^2}{(8K-1)\sin(\frac{\pi}{8K-1})}\left[\frac{\Gamma(1-\frac{1}{8K})}{\Gamma(\frac{1}{8K})}\right]^{8K/(8K-1)}}{\left[\Gamma\left(\frac{4K}{8K-1}\right)\Gamma\left(\frac{16K-3}{16K-2}\right)\right]^2}\right\}^{(8K-1)/(8K-2)}.$$

$$(3)$$

The parameters K, u, and A_x were obtained as functions of the magnetization S_z using DMRG on a single isolated chain by fitting the transverse correlation function (to get K and A_x [36]) and by deriving the magnetization curve to get the static susceptibility, $\chi = K/\pi u$, and thereby u (these TLL parameters are shown in SM [30]). In Fig. 2 we see that the TLL $S_\perp(T = 0)$ values considerably deviate from the DMRG+MF results, especially close to H_{c2}, while the two results should be identical in the $J_{ab}/J_c \ll 1$ limit. Apparently, as regards $S_\perp(T = 0)$, the value $J_{ab}/J_c \cong 1/12$ is not small enough to consider DTN as a system of *weakly* coupled spin chains and fully justify the TLL description, in particular when the *total* interchain coupling $Z J_{ab}$ becomes larger than the intrachain energy scale u close to H_{c2}. This is to be compared with other, more 1D compounds, such as BPCB, where the analytical TLL description of $S_\perp$ [17,18] was remarkably accurate and fully consistent with the numerical (DMRG+MF) treatment.

One may also wonder what is the orientation of the $S_\perp$ vector within the a-b plane (i.e., the phase of the complex order parameter) on each of the two tetragonal subsystems. When fitting the observed ^{14}N(2) NMR line splitting in the BEC phase (Fig. 2) we found several solutions for the orientation, which could not be clearly distinguished [30]. It turns out that for these different solutions the calculated proton spectra are quite different, and by comparing them to the experimentally observed one (not shown) we could determine the orientation of the $S_\perp$ vectors [28,30]. On both tetragonal subsystems $S_\perp$ is found to be approximately (within $\sim10°$) aligned perpendicularly to the in-plane component of the magnetic field (induced by the $3°$ tilt of H from the c axis). This orientation is indeed what is expected from the simplest model of classical spins subject to an easy-plane anisotropy. This means that the tilt of the field is the strongest source of axial symmetry breaking. Therefore, for a perfect sample alignment ($H \parallel c$ axis), we do expect that the symmetry requirement for the existence of a true BEC is fulfilled.

We now turn our attention to the *phase boundary* $T_c(H)$ (Fig. 3). By NMR the precise T_c value is detected from the peak position of the corresponding critical spin fluctuations. We measured it on the high-frequency proton ^{1}H(2) line as the corresponding peak of the transverse nuclear spin-spin relaxation rate $(1/T_2)$ or, equivalently, as the minimum intensity of the NMR signal recorded while varying H or T through the transition. From the same set of proton NMR measurements we also extracted the longitudinal spin component S_z *at the transition*, $S_z(T_c)$. This quantity, which relates to the critical boson density n_c (assuming holelike bosonic particles), $n_c = 1 - S_z(T_c)$, was accessed by the frequency shift of the ^{1}H(2) line $\delta f = \gamma A_{cc} g_c \mu_B S_z/(2\pi) = \widetilde{A}_{cc} S_z$, where A_{cc} is the relevant component of the hyperfine tensor (see SM [30]; $\widetilde{A}_{cc} = 2.98$ MHz).

In Fig. 3 we can see that QMC simulations are in excellent agreement with NMR data for both n_c and T_c (as was the case
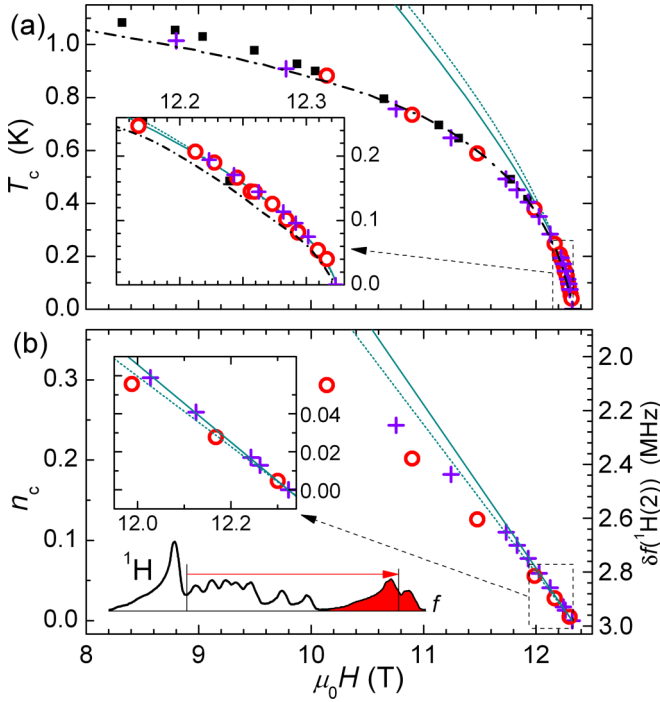
FIG. 3. NMR data (red circles) for (a) T_c and (b) the critical boson density n_c at T_c (see the text) are compared with theoretical predictions: QMC data points are shown as crosses, HFP predictions are given by the dotted and solid lines (for the parabolic and true magnon dispersion, respectively), and the TLL prediction for T_c [Eq. (4), with $k = 0.67$] by the dash-dotted line (see the text). In (a) squares correspond to the magnetocaloric effect data from Ref. [7] (with the field values downscaled by -2.3% to overlap the slightly different H_{c2} values). The lower inset in (b) explains the determination of the H(2) line-shift frequency (right scale in the main panel) that measures n_c. Other insets are zooms close to H_{c2}.

for $S_\perp$ in Fig. 2). T_c can also be described by the analytical TLL-based expression [17,18]

$$T_c = \frac{u}{2\pi}\left[\sin\left(\frac{\pi}{4K}\right)B^2\left(\frac{1}{8K},1-\frac{1}{4K}\right)\frac{kZJ_{ab}A_x}{u}\right]^{2K/(4K-1)},$$
(4)

where $B(X,Y) = \Gamma(X)\Gamma(Y)/\Gamma(X+Y)$, except very close to H_{c2} where the TLL description fails [16]. Here we have explicitly included a renormalization parameter k to take into account the effects of spin fluctuations beyond the MF treatment of interchain interaction. This was first discussed analytically for the Heisenberg spin chain in zero field in Ref. [37] and then precisely verified numerically in Ref. [38], where $k = 0.695$ was obtained. A slightly different value, $k = 0.74$ was successfully applied in describing $T_c(H)$ of

the BPCB compound [17,39], while for our DTN data we find $k = 0.67(2)$, pointing to a quite universal value of this correction.

Close to H_{c2} one expects that the 3D description of the HFP model, describing the low boson density limit, is valid. Using the low-energy quadratic approximation for the magnon dispersion [14], this model provides the canonical shape of the phase boundary, $T_c(H) \propto (H_{c2} - H)^{2/3}$, which is well observed by our NMR data, in contrast to previous reports [24]. (From a nonlinear power-law fit the exponent value is 0.72 ± 0.04.) To better access higher temperature, one can improve the model by taking the exact, numerically calculated dispersion of magnons (as in Ref. [40]), which indeed fits the data slightly better. In both cases, the interaction parameter $U_{3D} = g_c\mu_B(H_{c2} - H)/(2k_B n_c)$ was fitted to adapt the $T_c(H)$ data points below 0.25 K. The obtained values, $U_{3D} = 4.1$ and 3.7 K, are perfectly consistent with the initial slope of the measured $n_c(H)$ dependence shown in Fig. 3(b), confirming the validity of the HFP model. We remark that close to H_{c1} a higher value, $U_{3D} = 7.2$ K, was reported [25], which should be attributed to the renormalization described in Ref. [41]. In Fig. 3(a) we also see that the HFP model in both variants clearly fails above 0.3 K, corresponding to $n_c \cong 4\%$. We have verified that this cannot be compensated by taking the renormalized field-dependent U_{3D} value from the observed $n_c(H)$ dependence, meaning that above $n_c \cong 4\%$ the interactions modify the effective density of states as compared to its noninteracting value.

To conclude, by NMR we investigated static properties of the high-field part of the BEC phase in the quasi-1D quantum magnet DTN, and analyzed the data using several theoretical approaches. QMC numerical simulations for a standard spin-1 model provide excellent fit to the data, and we used them as a reference to discuss the applicability of other approximate techniques and their sensitivity to the strength of 3D coupling. For a moderately 1D system such as DTN ($J_c/J_{ab} \cong 12$) we find that analytical TLL-based predictions are still very good for T_c (when the renormalization of MF interaction is taken into account) but insufficient for the order parameter $S_\perp$. For $S_\perp$, DMRG+MF turns out to be precise, and does not require any renormalization. The HFP description is found to be valid only very close to H_{c2}, for the critical boson densities below 4%.

[1] S. Sachdev, *Quantum Phase Transition* (Cambridge University Press, Cambridge, UK, 2011).

[2] P. Coleman and A. J. Schofield, Nature (London) **433**, 226 (2005).

[3] S. Sachdev and B. Keimer, Phys. Today **64**(2), 29 (2011).

[4] Q. Si and F. Steglich, Science **329**, 1161 (2010).

[5] A. Paduan-Filho, R. D. Chirico, K. Joung, and R. L. Carlin, J. Chem. Phys. **74**, 4103 (1981).

[6] A. Paduan-Filho, X. Gratens, and N. F. Oliveira, Jr., Phys. Rev. B **69**, 020405(R) (2004).

[7] V. S. Zapf, D. Zocco, B. R. Hansen, M. Jaime, N. Harrison, C. D. Batista, M. Kenzelmann, C. Niedermayer, A. Lacerda, and A. Paduan-Filho, Phys. Rev. Lett. **96**, 077204 (2006).

[8] S. A. Zvyagin, J. Wosnitza, C. D. Batista, M. Tsukamoto, N. Kawashima, J. Krzystek, V. S. Zapf, M. Jaime, N. F. Oliveira, Jr., and A. Paduan-Filho, Phys. Rev. Lett. **98**, 047205 (2007).

[9] S. Mukhopadhyay, M. Klanjšek, M. S. Grbić, R. Blinder, H. Mayaffre, C. Berthier, M. Horvatić, M. A. Continentino, A. Paduan-Filho, B. Chiari, and O. Piovesana, Phys. Rev. Lett. **109**, 177206 (2012).

[10] N. Tsyrulin, C. Batista, V. S. Zapf, M. Jaime, B. R. Hansen, C. Niedermayer, K. C. Rule, K. Habicht, K. Prokes, K. Kiefer, E. Ressouche, A. Paduan-Filho, and M. Kenzelmann, J. Phys.: Condens. Matter **25**, 216008 (2013).

[11] E. Wulf, D. Hüvonen, R. Schönemann, H. Kühne, T. Herrmannsdörfer, I. Glavatskyy, S. Gerischer, K. Kiefer, S. Gvasaliya, and A. Zheludev, Phys. Rev. B **91**, 014406 (2015).

[12] T. Giamarchi, C. Rüegg, and O. Tchernyshyov, Nat. Phys. Lett. **4**, 198 (2008).

[13] I. Affleck, Phys. Rev. B **43**, 3215 (1991).

[14] T. Nikuni, M. Oshikawa, A. Oosawa, and H. Tanaka, Phys. Rev. Lett. **84**, 5868 (2000).

[15] V. Zapf, M. Jaime, and C. D. Batista, Rev. Mod. Phys. **86**, 563 (2014).

[16] T. Giamarchi and A. M. Tsvelik, Phys. Rev. B **59**, 11398 (1999).

[17] P. Bouillot, C. Kollath, A. M. Läuchli, M. Zvonarev, B. Thielemann, C. Rüegg, E. Orignac, R. Citro, M. Klanjšek, C. Berthier, M. Horvatić, and T. Giamarchi, Phys. Rev. B **83**, 054407 (2011).

[18] M. Klanjšek, H. Mayaffre, C. Berthier, M. Horvatić, B. Chiari, O. Piovesana, P. Bouillot, C. Kollath, E. Orignac, R. Citro, and T. Giamarchi, Phys. Rev. Lett. **101**, 137207 (2008).

[19] T. Hong, Y. H. Kim, C. Hotta, Y. Takano, G. Tremelling, M. M. Turnbull, C. P. Landee, H.-J. Kang, N. B. Christensen, K. Lefmann, K. P. Schmidt, G. S. Uhrig, and C. Broholm, Phys. Rev. Lett. **105**, 137207 (2010).

[20] M. Jeong, H. Mayaffre, C. Berthier, D. Schmidiger, A. Zheludev, and M. Horvatić, Phys. Rev. Lett. **111**, 106404 (2013).

[21] M. Jeong, D. Schmidiger, H. Mayaffre, M. Klanjšek, C. Berthier, W. Knafo, G. Ballon, B. Vignolle, S. Krämer, A. Zheludev, and M. Horvatić, Phys. Rev. Lett. **117**, 106402 (2016).

[22] T. Giamarchi, *Quantum Physics in One Dimension* (Oxford Science Publication, New York, 2004).

[23] M. Dupont, S. Capponi, and N. Laflorencie, Phys. Rev. B **94**, 144409 (2016).

[24] L. Yin, J. S. Xia, V. S. Zapf, N. S. Sullivan, and A. Paduan-Filho, Phys. Rev. Lett. **101**, 187205 (2008).

[25] A. Paduan-Filho, K. A. Al-Hassanieh, P. Sengupta, and M. Jaime, Phys. Rev. Lett. **102**, 077204 (2009).

[26] C. Slichter, *Principles of Magnetic Resonance*, 3rd ed. (Springer, New York, 1990).

[27] A. Abragam, *Principles of Nuclear Magnetism* (Oxford University Press, New York, 1961).

[28] R. Blinder, *Etude par Résonance Magnétique Nucléaire de Nouveaux États Quantiques Induits sous Champ Magnétique: Condensation de Bose-Einstein dans le Composé DTN*, Ph.D. thesis, Université Grenoble Alpes, 2015, available online at https://tel.archives-ouvertes.fr/tel-01235600.

[29] B. N. Figgis and P. A. Reynolds, J. Chem. Soc., Dalton Trans., 125 (1986).

[30] See Supplemental Material at http://link.aps.org/supplemental/10.1103/PhysRevB.95.020404 for details of the employed numerical techniques and NMR data analysis.

[31] However, the relative intensity of lines *within* the partial N(2) [or N(1)] spectra remains undistorted.

[32] S. R. White, Phys. Rev. Lett. **69**, 2863 (1992).

[33] S. R. White, Phys. Rev. B **48**, 10345 (1993).

[34] See ITensor library, http://itensor.org.

[35] The formulas in this Rapid Communication correspond to the expressions from Refs. [17,18] where we replaced the factor A_x by $2A_x$ as needed to switch from the spin-1/2 ladder to the spin-1 chain.

[36] T. Hikihara and A. Furusaki, Phys. Rev. B **69**, 064427 (2004).

[37] V. Yu. Irkhin and A. A. Katanin, Phys. Rev. B **61**, 6757 (2000).

[38] C. Yasuda, S. Todo, K. Hukushima, F. Alet, M. Keller, M. Troyer, and H. Takayama, Phys. Rev. Lett. **94**, 217201 (2005).

[39] B. Thielemann, Ch. Rüegg, K. Kiefer, H. M. Rønnow, B. Normand, P. Bouillot, C. Kollath, E. Orignac, R. Citro, T. Giamarchi, A. M. Läuchli, D. Biner, K. W. Krämer, F. Wolff-Fabris, V. S. Zapf, M. Jaime, J. Stahn, N. B. Christensen, B. Grenier, D. F. McMorrow, and J. Mesot, Phys. Rev. B **79**, 020408(R) (2009).

[40] G. Misguich and M. Oshikawa, J. Phys. Soc. Jpn. **73**, 3429 (2004).

[41] Y. Kohama, A. V. Sologubenko, N. R. Dilley, V. S. Zapf, M. Jaime, J. A. Mydosh, A. Paduan-Filho, K. A. Al-Hassanieh, P. Sengupta, S. Gangadharaiah, A. L. Chernyshev, and C. D. Batista, Phys. Rev. Lett. **106**, 037203 (2011).